Chemistry & Biology
Article

Natural Product-Derived Modulators of Cell Cycle Progression and Viral Entry by Enantioselective Oxa Diels-Alder Reactions on the Solid Phase

Torben Leßmann,[1,3,6] Michele G. Leuenberger,[1,3] Sascha Menninger,[1,3,6] Meritxell Lopez-Canet,[1,3] Oliver Müller,[2] Stefan Hümmer,[4,6] Jenny Bormann,[4,6] Kerstin Korn,[5,6] Eugenio Fava,[5,6] Marino Zerial,[5,6] Thomas U. Mayer,[4,6] and Herbert Waldmann[1,3,6,*]
[1] Abteilung Chemische Biologie
[2] Abteilung Strukturelle Biologie
Max-Planck-Institut für Molekulare Physiologie, Otto-Hahn-Strasse 11, 44227 Dortmund, Germany
[3] Chemische Biologie, Universität Dortmund, Fachbereich 3, 44227 Dortmund, Germany
[4] Abteilung Chemische Genetik, Max-Planck-Institut für Biochemie, Am Klopferspitz 18, 82152 Martinsried, Germany
[5] Max-Planck-Institut für Molekulare Zellbiologie und Genetik, Pfotenhauerstrasse 108, 01307 Dresden, Germany
[6] Chemical Genomics Centre of the Max-Planck Society, Otto-Hahn-Strasse 15, 44227 Dortmund, Germany
*Correspondence: herbert.waldmann@mpi-dortmund.mpg.de
DOI 10.1016/j.chembiol.2007.02.008

SUMMARY

The underlying frameworks of natural product classes with multiple biological activities can be regarded as biologically selected and prevalidated starting points in vast chemical structure space in the development of compound collections for chemical biology and medicinal chemistry research. For the synthesis of natural product-derived and -inspired compound collections, the development of enantioselective transformations in a format amenable to library synthesis, e.g., on the solid support, is a major and largely unexplored goal. We report on the enantioselective solid-phase synthesis of a natural product-inspired α,β-unsaturated δ-lactone collection and its investigation in cell-based screens monitoring cell cycle progression and viral entry into cells. The screens identified modulators of both biological processes at a high hit rate. The screen for inhibition of viral entry opens up avenues of research for the identification of compounds with antiviral activity.

INTRODUCTION

The identification of biologically active organic compounds is of utmost importance both for basic research and drug development. Besides the classical approach of identifying compounds by in vitro screens, i.e., by binding to an isolated protein, high-content cell-based screens have recently proven to be a powerful complementary approach [1–4]. Such a chemical-biological search strategy provides the advantage of selecting compounds that can act at multiple steps along a given biochemical pathway, monitored in a cellular context.

For this chemical-biological approach, compound classes need to be found that can be regarded as biologically prevalidated in vast chemical structure space, and efficient methods for their syntheses in a library format need to be devised. The search may be particularly yielding if links from such compound classes to the biological phenomena monitored in the respective cellular screens already exist (see below) [5, 6].

We have proposed to employ the frameworks of natural product classes as evolutionary selected and biologically prevalidated starting points in structural space for compound collection development [7–11] and developed a tree-like classification of the natural product frameworks identified in nature so far [11]. The biology-oriented synthesis (BIOS) of compound collections derived from these natural product frameworks provides a promising strategy in the search of new biologically active agents [12] and can be efficiently carried out on polymer-bound substrates, as they allow rapid diversification without intermediate purification steps.

Natural product-derived and -inspired compound collections have been synthesized on the solid support in a number of cases [13–24]. However, in order to meet the stereochemical demands of natural product frameworks, the use of enantioselective transformations on the solid phase presents a highly attractive though rarely addressed approach.

Here, we report on the enantioselective solid-phase synthesis of a natural product-inspired α,β-unsaturated δ-lactone collection and its investigation in cell-based screens monitoring cell cycle progression and viral entry into cells. This α,β-unsaturated δ-lactone motif belongs to the most frequently occurring scaffolds in nature [11] and is the characteristic underlying structural element of antiproliferative agents, immunosuppressants, and inhibitors for different enzymes, in particular protein phosphatases (see Figure 1) [25–30].

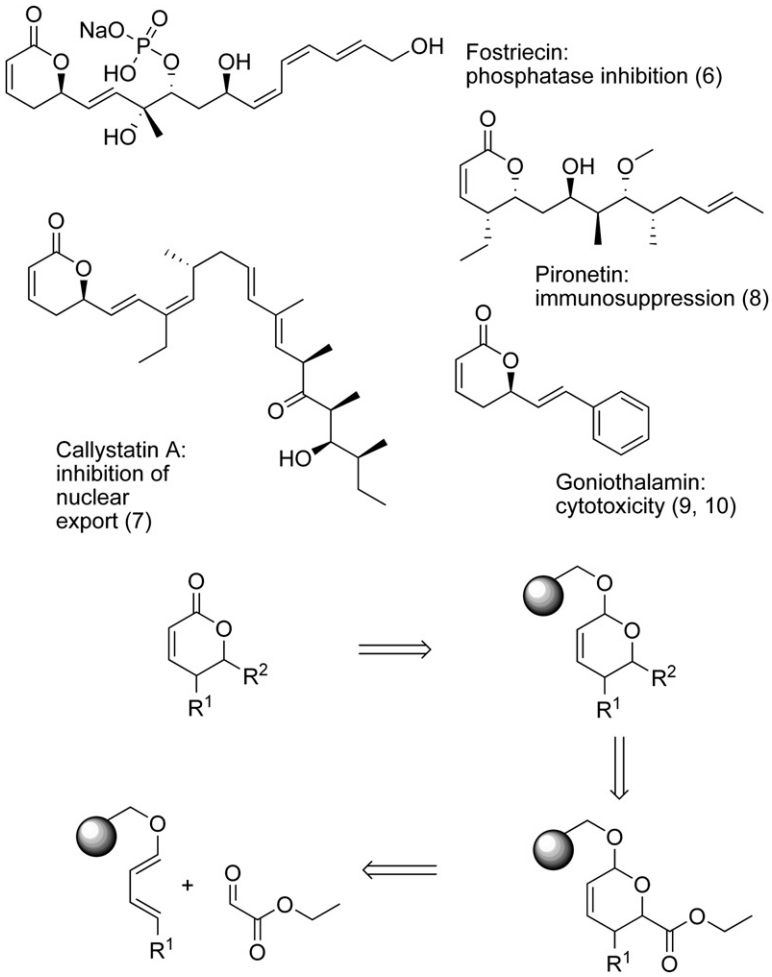

Figure 1. Structures of Natural Products Embodying the α,β-Unsaturated δ-Lactone Core Structure and Retrosynthetic Analysis for the Synthesis of α,β-Unsaturated δ-Lactones on the Solid Phase

RESULTS AND DISCUSSION

For the development of an asymmetric solid-phase synthesis of α,β-unsaturated δ-lactones we employed the enantioselective oxa Diels-Alder reaction between aldehydes and electron-rich 1-alkoxydienes [31–35] immobilized on the polymeric carrier as key stereodifferentiating transformation [36–40]. 1-Alkoxydienes were synthesized on the solid support and subjected to enantioselective cycloaddition with ethyl glyoxylate as the reactive heterodienophile (see Figure 1 for the retrosynthetic rationale). Subsequent derivatization of the ester followed by oxidation of the acetal cycloadduct to the lactone was supposed to give rise to a compound collection (see below) [13–26].

To this end, bromo-Wang polystyrene resin, **1** (loading 1.7 mmol·g^{-1}), was treated with the sodium salt of 3-hydroxyacrolein to yield polymer-bound α,β-unsaturated aldehyde, **2** (loading 1.0–1.6 mmol·g^{-1}, determined by titration with dinitrophenylhydrazine [17]), which was then transformed into immobilized dienes **3a**/**b** by means of a Wittig reaction (Figure 2). Next, the enantioselective hetero Diels-Alder reaction with ethyl glyoxylate was explored. After substantial experimentation, it was found that it proceeded with 90%–95% ee in the presence of 50 mol% Ti-(*R*)-BINOL complex **6** [31–33]. Methyl-substituted diene **3b** yielded only the *syn* isomer [41–44], with (*R*) configuration at C-6. The *syn* configuration was determined by comparison of the ^{1}H-NMR spectrum with data given in the literature [41–44]. The absolute and relative configurations of the cycloadducts were determined after release of the lactones from the resin and comparison of their specific rotations and characteristic NMR data with the corresponding values reported in the literature. After cleavage from the resin, compound **5a** was identical to the oxidation product of literature-known (*2R, 6S*)-6-methoxy-3,6-dihydro-2*H*-pyran-2-carboxylic acid ethyl ester (see [45]).

Release of the cycloadducts and oxidation to the lactones **5** was efficiently achieved in a single-step procedure by treatment of polymer-bound acetals **4** with the Jones reagent [46]. After flash chromatography, compounds **5** were isolated with >95% purity and in overall yields for the four-step sequence of 40% (**5a**) and 15% (**5b**), i.e., with 80% and 62% average yield per step.

For the synthesis of a compound collection, the ethyl ester was saponified on resin with LiOH [47] (Figure 2), and the resulting immobilized acids **7** were treated with different alkyl halides in the presence of cesium carbonate

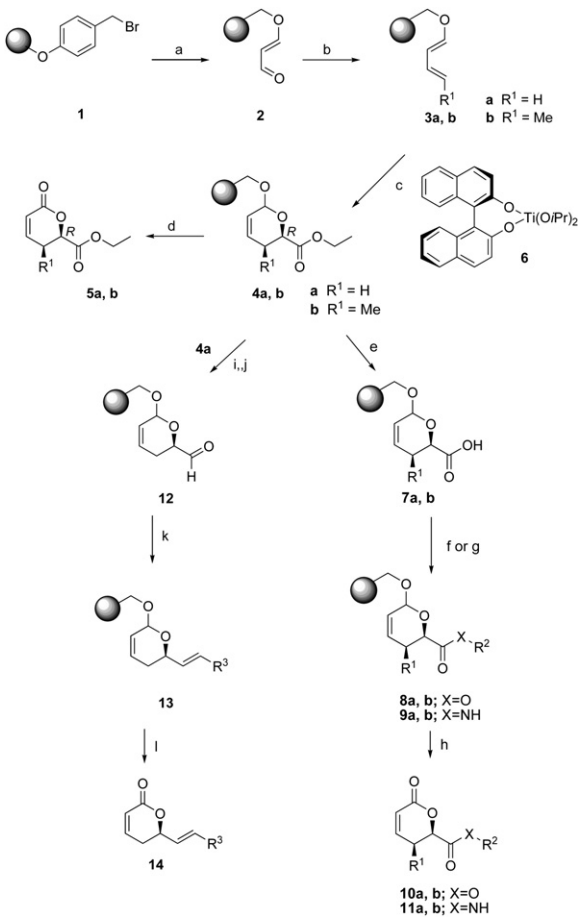

Figure 2. Solid-Phase Synthesis of the α,β-Unsaturated δ-Lactones

(a) Sodium-3-oxacrolein, DMF, rt, 18 hr, 65%–90%. (b) $MePh_3PBr$ or $EtPh_3PBr$, *n*-BuLi, THF, rt, 18 hr. (c) 50 mol% (Ti[(*R*)-BINOL][O*i*Pr]$_2$) (**6**), 10 equiv. ethyl glyoxylate, CH_2Cl_2, −30°C–0°C, 6 hr. (d) CrO_3, H_2SO_4, acetone/water, rt, 5 hr. (e) 20 equiv. LiOH, THF/water, rt, 5 hr. (f) 10–20 equiv. R^2-Br or R^2-Cl, 10–20 equiv. Cs_2CO_3, 0–1 equiv. NaI, DMF, rt, 24–144 hr. (g) 5 equiv. PyBOP, 10 equiv. DIEA, 5 equiv. H_2NR^2, DMF, rt, 2–5 hr. PyBOP, benzotriazole-1-yl-oxy-trispyrrolidino-phosphonium hexafluorophosphate; DIEA, *N,N*-diisopropylethyl-amine. (h) CrO_3, H_2SO_4, acetone/water, rt, 5 hr. (i) 4 equiv. $LiBH_4$, THF, 0°C to rt, 18 hr. (j) 4 equiv. IBX, THF/DMSO, rt, 20 hr. IBX, *o*-iodoxybenzoic acid. (k) 5 equiv. R^4PPh_3Br, 4.7 equiv. *n*-BuLi, THF, 0°C to rt, 18 hr. (l) 10–20 equiv. CrO_3, H_2SO_4, acetone/water, rt, 5 hr.

[48, 49] to finally deliver esters **10** in ca. 50% (aliphatic halides) to ca. 80% (benzyl halides and α-halocarboxylic acid esters) yield. Similarly, amides **11** were obtained in yields of ca. 50% after activation of the carboxylic acids with PyBOP (Figure 2). Notably, neither the nucleophilic ester formation nor the activation in the course of the amide synthesis affected the stereoisomer ratio initially established during the cycloaddition. α,β-Unsaturated δ-lactones **10** and **11** were isolated with purities typically >90% after flash chromatography or purification by preparative reverse-phase HPLC on a C18 column. A selection of representative examples is shown in Table 1 (see Table S1 in the Supplemental Data available with this article online for a list of structures and yields of all compounds synthesized).

In order to more closely approximate the structure of the guiding natural products, ester **4a** was converted into immobilized aldehyde **12**, which was then subjected to a Wittig reaction with different phosphonium salts. Olefins **14** were finally released from the solid support by again employing the Jones oxidation protocol. The double bond next to the lactone ring resembles the core structure of various naturally occurring α,β-unsaturated δ-lactones (Figure 1), and, in fact, goniothalamin (see Table 1) and several related compounds (see the Supplemental Data) were obtained by this solid-phase procedure.

By means of the sequence of syntheses detailed above, a collection of 50 compounds was synthesized.

In order to test for biological activity, the synthesized compound collection was subjected to the aforementioned cell-based screens.

Pironetin (Figure 1) arrests cell cycle progression in M phase and is a potent inhibitor of tubulin assembly [50–52], indicating a possible link between this biological process and α,β-unsaturated δ-lactones.

Therefore, the synthesized compounds were subjected to a phenotypic cell-based screen monitoring their influence on cell cycle progression. In this screen, BSC-1 cells (from African green monkey) cultured in 384-well plates were treated for 8 hr with 30 μM of the synthesized compounds. This cell line was chosen due to its proven advantage in assessing the influence of chemical compounds on the cell cycle [53]. Treated cells were fixed with formaldehyde and stained for chromatin and the actin- and microtubule cytoskeleton. Microscopic analysis revealed that several of the investigated compounds influenced the microtubule cytoskeleton in dividing and/or nondividing cells. Closer examination of the compound-induced phenotypes revealed that, for example, **10a/10** and **11a/1** induced the formation of bipolar spindles with a high frequency of misaligned chromosomes (see Figure 3). The pole-to-pole distance of spindles observed in cells treated with 100 μM **10a/10** appeared to be greater than in DMSO-treated cells (see Figure 3A), suggesting that these compounds might affect proteins involved in regulating spindle morphology. At this concentration, **10a/10** also affected the actin cytoskeleton, as shown in Figure 3. While **10a/10** induced the formation of larger spindles, **11a/1** did not affect spindle length, but caused severe defects in chromosome alignment (see Figure 3). Additionally, **11a/1**-treated cells displayed a bent spindle phenotype with curvy and disorganized microtubules, indicating that **11a/1**, like **10a/10**, might affect microtubule dynamics. As evident from Figure 3, compound **11a/1**, unlike **10a/10**, did not affect the actin cytoskeleton. To confirm that the observed cellular phenotypes were mediated by **10a/10** and **11a/1** rather than by possible decomposition products cells were treated with benzyl alcohol and alanine methyl ester, the products of eventual intracellular esterase or peptidase cleavage. Intriguingly, these compounds had no effect on either the actin- or microtubule cytoskeleton, confirming that **10a/10** and **11a/1** account

Table 1. Selected α,β-Unsaturated δ-Lactones Obtained by Enantioselective Solid-Phase Synthesis

Entry	Compound	Structure
1	**10a/1**	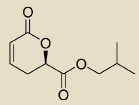
2	**10a/2**	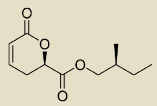
3	**10a/3**	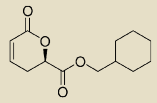
4	**10a/4**	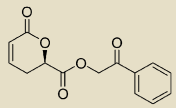
5	**10a/5**	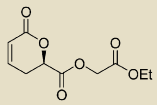
6	**10a/10**	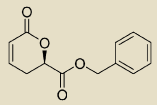
7	**10a/12**	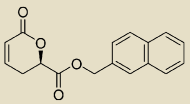
8	**10b/9**	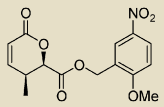
9	**10b/21**	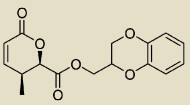
10	**11a/1**	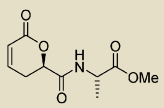
11	**11b/1**	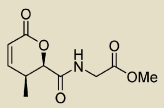
12	**11b/2**	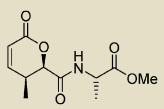

Table 1. *Continued*

Entry	Compound	Structure
13	**14/1**	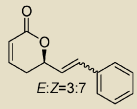 Goniothalamin
14	**14/5**	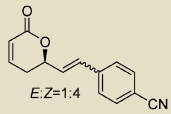

for the observed cellular effects. Since both compounds induced defects in microtubule morphology, in vitro assays were performed to analyze the effect of **10a/10** and **11a/1** on microtubule polymerization. To this end, tubulin purified from pig brain was induced to polymerize in the presence of GTP by incubating it at 30°C in the presence of **10a/10**, **11a/1**, DMSO as a solvent control, or the microtubule poison nocodazole [54]. To obtain a quantitative readout, we monitored microtubule polymerization by measuring the turbidity of the reaction at 350 nm. As shown in Figure S1, tubulin efficiently polymerized into microtubule polymers in the presence of DMSO, as evident from the fact that the absorbance constantly increased until it started to plateau about 12 min after the start of the reaction. To confirm that microtubule polymer, but not protein aggregates, account for the observed increase in absorbance, reactions were cooled to 15°C after 25 min (black triangle in Figure S1) to induce microtubule depolymerization. As expected, the cold treatment rapidly induced a decrease in absorption, confirming that the turbidity was mediated by microtubule polymer. Both **10a/10** and **11a/1** had a reproducible inhibitory effect on microtubule polymerization at a concentration of 80 μM (see Figure S1, each compound was tested in duplicate). Notably, **5b** (Table S1) which is structurally related to **10a/10** and **11a/1** but did not affect the cytoskeleton in cells, had no significant effect on microtubule polymerization in vitro, indicating that there is a correlation between the cellular phenotype and the inhibitory activity on microtubule polymerization in vitro. At higher concentration, both compounds were less efficient in inhibiting microtubule polymerization (data not shown), indicating that **10a/10** and **11a/1** might not be soluble at high concentrations. Therefore, the IC_{50} values of **10a/10** and **11a/1** on microtubule polymerization could not be determined. Compared to nocodazole, both compounds were less efficient in inhibiting microtubule polymerization in vitro (see Figure S1), suggesting that the observed cellular effects of **10a/10** and **11a/1** upon the microtubule cytoskeleton might not be exclusively mediated by their inhibitory effect on microtubule polymerization. Further work will be required to address questions of potencies, selectivities, and mode of mechanisms of the compounds **10a/10** and **11a/1**. Since spindle-associated proteins and microtubules are promising targets for chemical biology

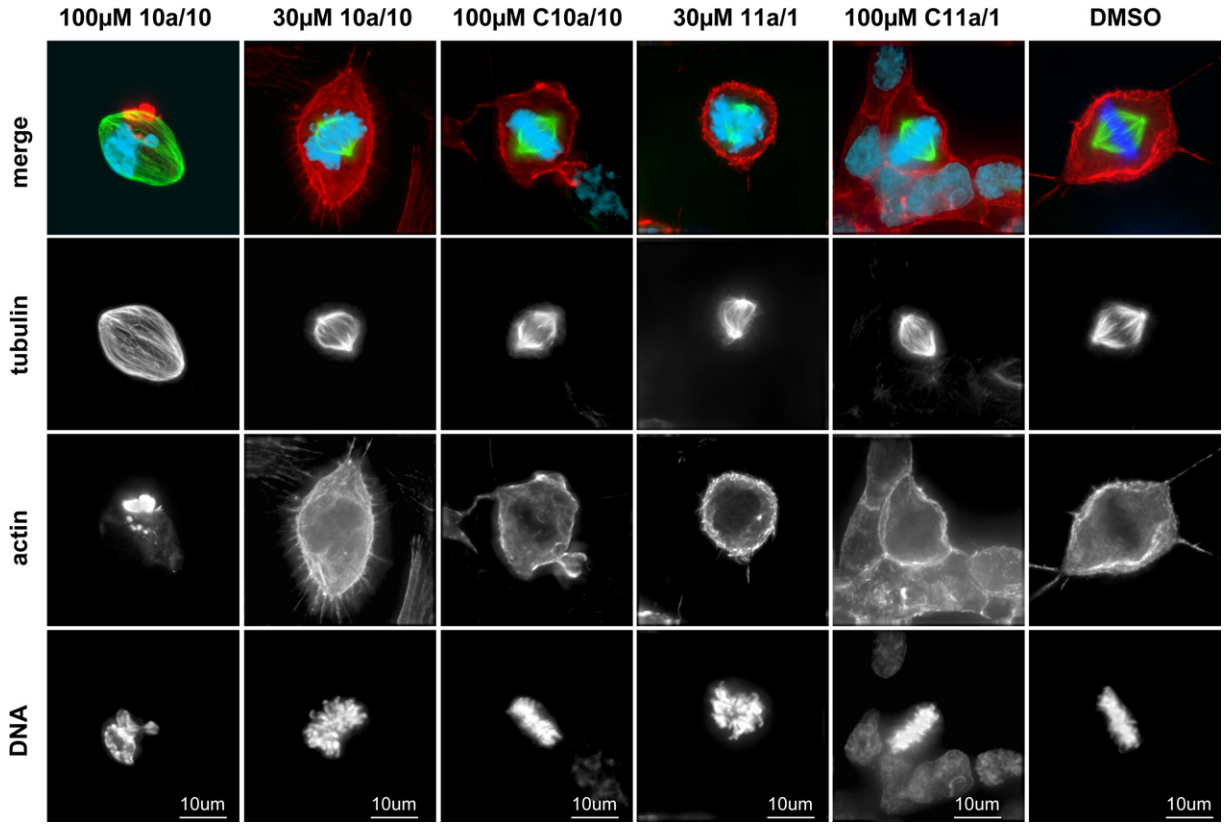

Figure 3. Results of the Assay for Influence on the Progression of the Cell Cycle
Immunofluorescent images of BSC-1 cells treated with compounds **10a/10**, **C10a/10** (benzyl alcohol), **11a/1**, and **C11a/1** (alanine methyl ester). Chromatin-, actin-, and microtubule structures are shown individually and as an overlay colored in blue, red, and green, respectively.

research and drug development [55], these studies might open up new avenues of research in these areas of investigation.

The second cell-based screen exploits the property of vesicular stomatitis virus (VSV) to hijack the endocytic pathway to infect host cells. VSV enters via clathrin-mediated endocytosis and is transported to early and late endosomes (see Figures 4A and 4B). This assay has recently been used to explore genome-wide the function of kinases at various steps of the clathrin-mediated endocytic route by RNA interference (RNAi); this assay was performed in HeLa cells and uncovered an unexpected complexity of regulation of protein, lipid, and carbohydrate phosphorylation in this biological process [56]. Given that the natural products based on α,β-unsaturated δ-lactones are also functionally related to protein phosphorylation (see above), and that kinases and phosphatases may have both activating and inactivating functions, we probed the activity of the synthesized compounds by using this cell-based assay validated for human kinases. Infection of HeLa cells by a recombinant VSV-expressing GFP (rVSP-GFP) in the presence of individual compounds (30 μM) was monitored by imaging GFP expression in 96-well plates by using a fully automated confocal microscope (Figure 4C).

Four different fields per well were imaged for GFP and DRAQ5 for staining of nuclei. From each field, the number of infected cells (the GFP channel) out of total cells (DRAQ5) was determined by using an automated image-analysis algorithm. The average number of infected cells in each well and, from these, the total average were calculated. By dividing the number of infected cells by the number of infected cells from negative control wells, the relative VS infection index was calculated, as described [56]. The relative cell number was obtained by dividing the number of cells by the number of cells from negative control wells. All data were collected in two independent experiments.

Positive hits were considered when the relative VSV infection index was reduced or enhanced at least 3-fold in the presence of the respective compound, as described [56].

A total of eight α,β-unsaturated δ-lactones reduced virus infectivity and the relative cell number at least 3-fold (Figure 4D). An increase in virus infectivity was not observed. Notably, four of these compounds (Figure 4D) reduced virus infectivity but did not lower the relative cell number below the threshold. Three compounds, namely, **10a/8**, **10a/14**, and **10b/10**, did exclusively score in this screen, indicating selectivity. Comparison of the structures of these two groups of compounds suggests that

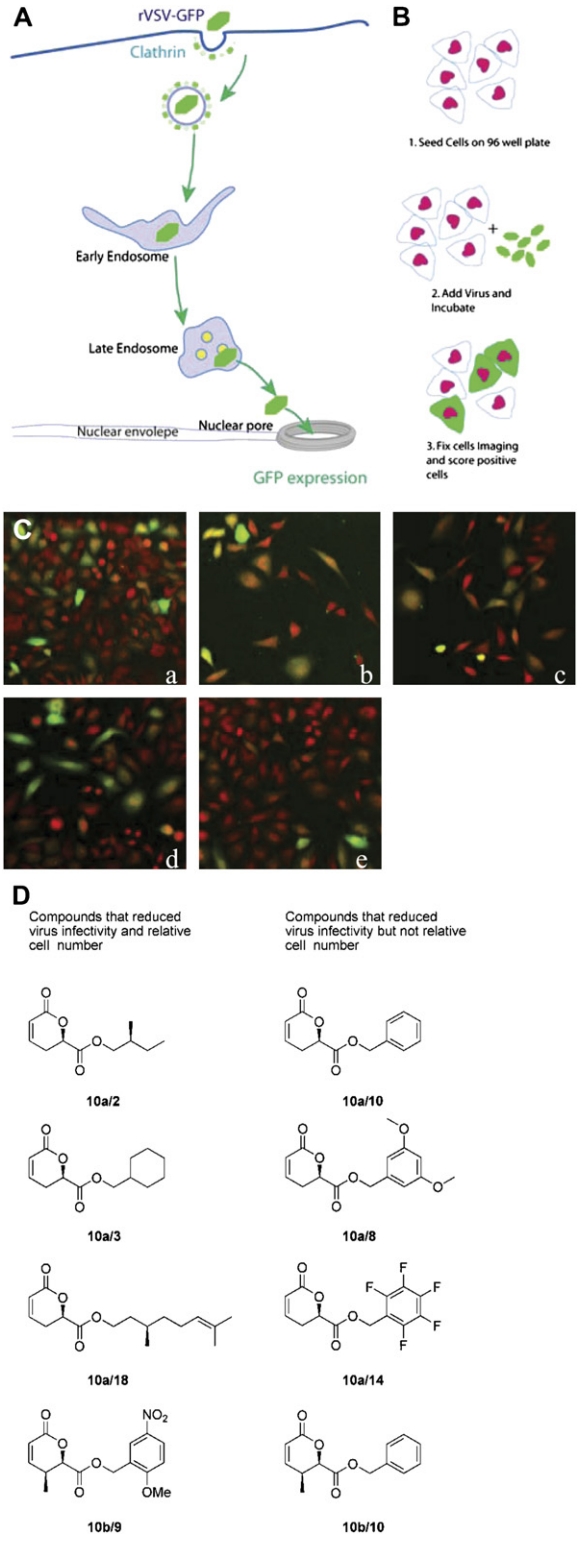

Figure 4. rVSV-GFP Infectivity Assay

(A and B) Schematic illustration of the assay principle.

(C) Images acquired in the screen: (a) control, (b) **10a/10**, (c) **10b/10**, (d) **11a/2**, and (e) **10a/14**; note that the amide **11a/2** did not score in the screen.

(D) Structures of the compounds identified as hits in the screen.

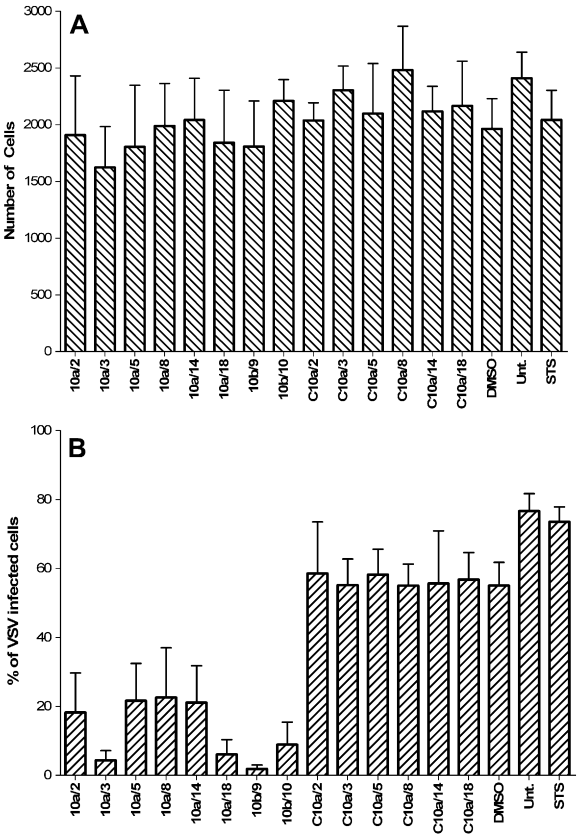

Figure 5. Comparison of Active Esters with the Correspondent Alcohols

(A) Cell scoring in HeLa cells treated with active ester and corresponding alcohols does not show any major difference from untreated cells, indicating an absence of acute cytotoxicity during the experimental window.

(B) VSV infectivity of cells is strongly reduced in HeLa cells treated with the active esters, but it is not significantly changed in HeLa cells treated with the alcohols. C…, control substance (i.e., corresponding alcohol); Unt., untreated; STS, staurosporine.

Error bars indicate the standard deviations for the measurements.

an aromatic residue in the side chain of the lactones may be beneficial for the selective mode of action. Also, amides were not active (also see Figure 4D).

In order to further investigate the specificity of the compounds under physiological conditions, the selected positive hits were again compared with their potential cleavage products (i.e., alcohols). HeLa cells incubated with esters and alcohols were infected by using VSV, and the infection rate was determined (Figure 5). The results clearly show that whereas all esters reduced VSV infectivity, their respective alcohols failed, indicating that the α,β-unsaturated δ-lactone moiety is essential for activity. Additionally, the data show that an even shorter incubation time (2 hr) is sufficient to protect cells from viral infection; the active compounds are stable at least during this period of time (see the Supplemental Data).

Finally, we found that the known apoptosis-inducing compound staurosporine did not affect the number of

infected cells compared to control samples (Figure 5), excluding the possibility that the effect of the active α,β-unsaturated δ-lactones is due to induction of cell death and consequent impairment of basic physiological functions.

Several signaling pathways involving phosphorylation events, particularly the cell growth TOR, the MAP kinase, the Ca^{2+}, and the actin turnover pathways, have been shown to require or stimulate clathrin-mediated endocytosis [56]. Interestingly, ablation of several of the kinases identified in the kinome survey displayed strictly pathway-specific effects on cell viability and proliferation. Given the known connection between the phosphatase-inhibiting activity of several of the guiding natural products (see above) and the antagonizing effects of phosphatases and kinases, it is conceivable that the compounds identified to specifically inhibit VSV infection (i.e., without affecting cell number) may act upon a subset of protein phosphatases and/or kinases acting on this endocytic pathway. In this respect, the siRNA kinome-wide screen [56] offers a number of suitable candidates.

These initial results demonstrate that the methodology developed by us offers a new, to our knowledge, principle for screening small molecules in the field of viral infection. In particular, the combination of this screening method with genome-wide RNAi screens should provide an efficient means for identification of novel regulatory pathways, novel targets within these pathways, as well as chemical modulators acting upon them.

In conclusion, we demonstrate that highly enantioselective oxa Diels-Alder reactions with solid-phase, bound dienes can successfully be carried out by employing a chiral titanium catalyst. Elaboration of the cycloadducts into a compound collection resembling naturally occurring α,β-unsaturated δ-lactones was successfully achieved.

This collection proved to yield new, to our knowledge, modulators of cell cycle progression and viral entry into cells at a high hit rate in cell-based assays and thereby may open up new avenues of research. The natural product-derived α,β-unsaturated δ-lactone moiety was essential for the observed effects in all cases. We note that the screen monitoring viral entry in general provides an unprecedented opportunity for the identification of novel classes of antiviral compounds.

SIGNIFICANCE

The use of small molecules for the study of biological phenomena is of major interest to chemical biology and medicinal chemistry research. For such endeavors, compound classes that can be regarded as relevant to biology, that are amenable to compound collection development, and that yield high hit rates at a comparably small library size are required.

In order to develop compound collections that meet these criteria, we propose to employ classes of natural products with prevalidated biological relevance as starting points in structure space. The effort required for the synthesis of such compound collections exceeds the set of transformations typically employed in combinatorial chemistry; in particular, enantioselective transformations are needed. Here, we present the development of enantioselective oxa Diels-Alder reactions for the synthesis of natural product-inspired compound collections in a format amenable to compound library synthesis. Hetero Diels-Alder reactions catalyzed by a chiral titanium complex were employed to obtain a collection of 50 α,β-unsaturated δ-lactones, a structural motif present in various biologically active natural products.

The resulting compound collection was subjected to biological evaluation in phenotype-based screens and yielded new, to our knowledge, modulators of cell cycle progression and inhibitors of viral entry into cells.

EXPERIMENTAL PROCEDURES

A record of all experimental procedures and characterization of representative compounds is given in the Supplemental Data.

General Procedure for Diene Formation on the Solid Support

The phosphonium salt (3 equiv.) was suspended in 10 ml dry THF, and a solution of *n*-BuLi (1.6 M in hexane, 2.9 equiv.) was slowly added. The deep-red solution was added to the polymer-bound aldehyde (5 g, 5.84 mmol) in 20 ml dry THF. The mixture was shaken for 12 hr at room temperature. The resin was filtered, washed with 3:1 THF:H_2O (50 ml), THF (100 ml), DMF (50 ml), MeOH (30 ml), and CH_2Cl_2 (100 ml), and dried in vacuo. The completion of the reaction was confirmed by monitoring the disappearance of the C=O band in the IR.

General Procedure for the Hetero Diels-Alder Reaction on the Solid Support

(*R*)-BINOL (1.7 mmol, 1 equiv.) was dissolved in 7.5 ml dry CH_2Cl_2, and a solution of $Ti(OiPr)_4$ (0.85 mmol, 0.5 equiv.) in 2.5 ml dry CH_2Cl_2 was added. The mixture was heated to reflux for 1 hr, then evaporated and dried in vacuo for 1.5 hr. The catalyst dissolved in 10 ml dry CH_2Cl_2 was added to the suspension of the polymer-bound diene (1 g, 1.7 mmol) in 10 ml dry CH_2Cl_2 that was cooled to −30°C. Freshly distilled ethyl glyoxylate (10 equiv.) was added in small amounts over the course of 3 hr at a constant temperature of −30°C. The mixture was allowed to warm up to 0°C over the course of 2hr. The resin was filtered, washed with CH_2Cl_2 (20 ml), DMF (20 ml), 1:1 DMF:H_2O (25 ml), DMF (25 ml), MeOH (20 ml), and CH_2Cl_2 (50 ml), and dried in vacuo. After the cleavage of a small amount (100 mg), the loading resulted in 0.4–0.1 mmol/g (30%–10%).

Cell Cycle Progression Screen

BSC-1 (African green monkey) cells were cultured in 384-well plates at a density of about 1500 cells per well. Compounds dissolved in DMSO were transferred by a robot-controlled pin array to a final concentration of about 30 μM. BSC-1 cells treated for 8 hr with the synthesized compounds or an equivalent volume of DMSO were fixed with 4% formaldehyde (80 mM PIPES [pH 6.8], 1 mM MgCl2, 1 mM EGTA, 0.1% Triton X-100) and were stained for microtubules, actin, and chromatin with FITC-labeled anti-tubulin antibodies (Sigma), TRITC-labeled Phalloidin (Sigma), and Hoechst (Sigma), respectively. Images were acquired on an automated microscope (Zeiss 200M) equipped with a 20× lens. High-quality images were acquired on a Nikon T200 inverted fluorescence microscope and were deconvolved by using Applied Precision software.

rVSV-GFP Infectivity Assay

HeLa cells (human cervix carcinoma cell line) were obtained from DSMZ, Braunschweig and maintained in D-MEM medium (GIBCO-BRL) without phenol red supplemented with 10% fetal calf serum

(FCS), 2 mM L-glutamine, and 1% penicillin-streptomycin. The cell number was determined with a CASY cell counter (Schärfe System GmBH, Reutlingen). The cells were incubated at 37°C in 5% CO_2 and were seeded by using the Multidrop 384 dispenser (Thermo). On day 0, 4000 HeLa cells were plated in 80 μl complete medium in 96-well (3619, Corning) plates and were incubated at 37°C and 5% CO_2 overnight. At day 1, compounds were added to the cells at a final concentration of 30 μM and were incubated. After 18 hr, rVSV-GFP was added to the cells. To assure specific pathway entry of the virus, a multiplicity of infection (MOI) of 0.1 was used in the experiment. After the infection period of 4 hr, 50 μl 16% formaldehyde in PBS was added, and the cells were fixed for at least 20 min. Nuclei were stained with DRAQ5, and samples were imaged.

To assess the effect of the ester's potential cleavage products, HeLa cells were incubated with both lactone esters and their corresponding alcohols for 2 hr. After this time, cells were infected with VSV for 3 hr (the time necessary to obtain expression of GFP). Cells were then fixed and processed as described above. Samples were done in duplicate, and the experiments were repeated twice. Results were calculated for each experiment as the average of the duplicate and its standard deviation (intraexperiment variation). Finally, results of the two independent experiments were compared as the average of the experiment and its standard deviation (interexperiment variation).

In control samples, an average number of cells of 1000 were detected. Images were acquired with a 10× lens and an automated confocal microscope (OPERA, Evotec Technologies, Hamburg, Germany).

Supplemental Data

Supplemental Data include descriptions of additional general reaction procedures, a list of all synthesized compounds with the results of the syntheses, data for characterization of representative examples for α,β-unsaturated δ-lactones, a description of the tubulin polymerization assay, and the results of the viral entry screen and are available at http://www.chembiol.com/cgi/content/full/14/4/443/DC1/.

ACKNOWLEDGMENTS

This research was supported by the Max-Planck-Society, the Deutsche Forschungsgemeinschaft, and the Fonds der Chemischen Industrie. We are grateful to Lucas Pelkmans for the VSV infection cell screen system. We would like to thank Eberhard Krausz, Ivan Baines, and all members in the High-Throughput Technology Development Studio (HT-TDS) at MPI-CBG for their support and contributions to the experiments in the VSV screen.

Received: February 28, 2006
Revised: January 31, 2007
Accepted: February 9, 2007
Published: April 27, 2007

REFERENCES

1. Stockwell, B.R. (2004). Exploring biology with small organic molecules. Nature *432*, 846–854.
2. Bredul, M., and Jacoby, E. (2004). Chemogenomics: an emerging strategy for rapid target and drug discovery. Nat. Rev. Genet. *5*, 262–275.
3. Berg, T. (2005). Cellular profiling of small-molecule bioactivities: an alternative tool for chemical biology. Angew. Chem. Int. Ed. *44*, 5008–5011.
4. Mitchison, T.J. (2005). Small-molecule screening and profiling by using automated microscopy. ChemBioChem *6*, 33–39.
5. Müller, O., Gourzoulidou, E., Carpintero, M., Karaguni, I.-M., Langerak, A., Herrmann, C., Möröy, T., Klein-Hitpaß, L., and Waldmann, H. (2004). Identification of potent Ras signalling inhibitors by pathway-selective phenotype-based screening. Angew. Chem. Int. Ed. *43*, 450–454.
6. Waldmann, H., Karaguni, I.-M., Carpintero, M., Gourzoulidou, E., Herrmann, C., Brockmann, C., Oschkinat, H., and Müller, O. (2004). Sulindac-derived Ras pathway inhibitors target the Ras-Raf interaction and downstream effectors in the Ras pathway. Angew. Chem. Int. Ed. *43*, 454–458.
7. Breinbauer, R., Vetter, I.R., and Waldmann, H. (2002). From protein domains to drug candidates – natural products as guiding principles in the design and synthesis of compound libraries. Angew. Chem. Int. Ed. *41*, 2878–2890.
8. Koch, M.A., and Waldmann, H. (2005). Protein structure similarity clustering and natural product structure as guiding principles in drug discovery. Drug Discov. Today *10*, 471–482.
9. Koch, M.A., Wittenberg, L.O., Basu, S., Jeyaraj, D.A., Gourzoulidou, E., Reinecke, K., Odermatt, A., and Waldmann, H. (2004). Compound library development guided by protein structure similarity clustering and natural product structure. Proc. Natl. Acad. Sci. USA *101*, 16721–16726.
10. Charette, B.D., MacDonald, R.G., Wetzel, S., Berkowitz, D.B., and Waldmann, H. (2006). Protein structure similarity clustering. Angew. Chem. Int. Ed. *45*, 7766–7770.
11. Koch, M.A., Schuffenhauer, A., Scheck, M., Wetzel, S., Casaulta, M., Odermatt, A., Ertl, P., and Waldmann, H. (2005). Charting biologically relevant chemical space: a structural classification of natural products (SCONP). Proc. Natl. Acad. Sci. USA *102*, 17272–17277.
12. Nören-Müller, A., Reis-Corrêa, I., Jr., Prinz, H., Rosenbaum, C., Saxena, K., Schwalbe, H.J., Vestweber, D., Cagna, G., Schunk, S., Schwarz, O., et al. (2006). Discovery of protein phosphatase inhibitor classes by biology-oriented synthesis. Proc. Natl. Acad. Sci. USA *103*, 10606–10611.
13. Nicolaou, K.C., Winssinger, N., Pastor, J., Ninkovic, S., Sarabia, F., He, Y., Vourloumis, D., Yang, Z., Li, T., Gainnakakou, P., and Hamel, E. (1997). Synthesis of epothilones A and B in solid and solution phase. Nature *387*, 268–272.
14. Nicolaou, K.C., Pfefferkorn, J.A., and Cao, G.-Q. (2000). Selenium-based solid-phase synthesis of benzopyrans I: applications to combinatorial synthesis of natural products. Angew. Chem. Int. Ed. *39*, 734–739.
15. Dragoli, D.R., Thompson, L.A., O'Brien, J., and Ellman, J.A. (1999). Parallel synthesis of prostaglandin E_1 analogues. J. Comb. Chem. *1*, 534–539.
16. Barun, O., Sommer, S., and Waldmann, H. (2004). Asymmetric solid-phase synthesis of 6,6-spiroketals. Angew. Chem. Int. Ed. *44*, 3195–3199.
17. Brohm, D., Philippe, N., Metzger, S., Bhargava, A., Müller, O., Lieb, F., and Waldmann, H. (2002). Solid-phase synthesis of dysidiolide-derived protein phosphatase inhibitors. J. Am. Chem. Soc. *124*, 13172–13178.
18. Arya, P., Joseph, R., Gan, Z., and Rakic, B. (2005). Exploring new chemical space by stereocontrolled diversity-oriented synthesis. Chem. Biol. *12*, 163–180.
19. Ortholand, J.-Y., and Ganesan, A. (2004). Natural products and combinatorial chemistry: back to the future. Curr. Opin. Chem. Biol. *8*, 271–280.
20. Boldi, A.M. (2004). Libraries from natural product-like scaffolds. Curr. Opin. Chem. Biol. *8*, 281–286.
21. Sanz, M.A., Voigt, T., and Waldmann, H. (2006). Enantioselective catalysis on the solid phase: synthesis of natural product-derived tetrahydropyrans employing the enantioselective oxa-Diels-Alder reaction. Adv. Synth. Catal. *348*, 1511–1514.
22. Sommer, S., and Waldmann, H. (2005). Solid phase synthesis of a spiro[5.5]ketal library. Chem. Commun. 5684–5686.

23. García, A.B., Leßmann, T., Umayre, J.D., Mamane, V., Sommer, S., and Waldmann, H. (2006). Stereocomplementary synthesis of a natural product-derived compound collection on a solid phase. Chem. Commun. 3868–3870.
24. Meseguer, B., Alonso-Diaz, D., Griebenow, N., Herget, T., and Waldmann, H. (1999). Natural product synthesis on polymeric supports - synthesis and biological evaluation of an indolactam library. Angew. Chem. Int. Ed. *38*, 2902–2906.
25. Lewy, D.S., Gauss, C.-M., Soenen, D.R., and Boger, D.L. (2002). Fostriecin: chemistry and biology. Curr. Med. Chem. *9*, 2005–2032.
26. Kalesse, M., and Christmann, M. (2002). The chemistry and biology of the Leptomycin family. Synthesis 981–1003.
27. Watanabe, H., Watanabe, H., Bando, M., Kido, M., and Kitahara, T. (1999). An efficient synthesis of pironetins employing a useful charal building block, (*1S, 5S, 6R*)-5-hydroxybicyclo[4.1.0]reptan-2-one. Tetrahedron *55*, 9755–9776.
28. Ramachandran, P.V., Reddy, M.V.R., and Brown, H.C. (2000). Asymmetric synthesis of goniothalamin, hexadecanolide, massoia lactone, and parasorbic acid via sequential allylboration ring-closing metathesis reactions. Tetrehedron Lett. *41*, 583–586.
29. Collett, L.A., Davies, M.T., and Rivett, D.E.A. (1998). Naturally occurring 6-substituted 5,6-dihydro-α-pyrones. Fortschr. Chem. Org. Naturst. *75*, 182–209.
30. Davies, M.T., and Rivett, D.E.A. (1989). Naturally occurring 6-substituted 5,6-dihydro-α-pyrones. Fortschr. Chem. Org. Naturst. *55*, 1–35.
31. Mikami, K., Motoyama, Y., and Terada, M. (1994). Asymmetric catalysis of Diels-Alder cycloadditions by an MS-free binaphthol-titanium complex: dramatic effect of MS, linear vs. nonlinear relationship, and synthetic applications. J. Am. Chem. Soc. *116*, 2812–2820.
32. Christmann, M., Bhatt, U., Quitschalle, M., Claus, E., and Kalesse, M. (2000). Total synthesis of (+)-ratjadone. Angew. Chem. Int. Ed. *39*, 4364–4366.
33. Quitschalle, M., Christmann, M., Bhatt, U., and Kalesse, M. (2001). Synthesis of unsaturated lactone moieties by asymmetric hetero Diels-Alder reactions with binaphthol-titanium complexes. Tetrahedron Lett. *42*, 1263–1265.
34. Dossetter, A.G., Jamison, T.F., and Jacobsen, E.N. (1999). Highly enantio- and diastereoselective hetero-Diels-Alder reactions catalyzed by new chiral tridentate chromium (III) catalysts. Angew. Chem. Int. Ed. *38*, 2398–2400.
35. Chavez, D.E., and Jacobsen, E.N. (2001). Total synthesis of fostriecin (CI-920). Angew. Chem. Int. Ed. *40*, 3667–3670.
36. Yli-Kauhaluoma, J. (2001). Diels-Alder reactions on solid supports. Tetrahedron *57*, 7053–7071.
37. Dujardin, G., Leconte, S., Coutable, L., and Brown, E. (2001). $Eu(fod)_3$-catalyzed solid-phase [4+2] heterocycloadditions: an efficient asymmetric process in catalyst-recycling conditions. Tetrahedron Lett. *42*, 8849–8852.
38. Stavenger, R.A., and Schreiber, S.L. (2001). Asymmetric catalysis in diversity-oriented organic synthesis: enantioselective synthesis of 4320 encoded and spatially segregated dihydropyranocarboxamides. Angew. Chem. Int. Ed. *40*, 3417–3421.
39. Kurosu, M., Porter, J.R., and Foley, M.A. (2004). An efficient synthesis of indane-derived bis(oxazoline) and its application to hetero Diels-Alder reactions on polymer support. Tetrahedron Lett. *45*, 145–148.
40. Leßmann, T., and Waldmann, H. (2006). Enantioselective synthesis on the solid phase. Chem. Commun. 3380–3389.
41. Bialy, L., Lopez-Canet, M., and Waldmann, H. (2002). Determination of the relative configuration of the C-2-C-1′-fragment of cytostatin. Synthesis 2096–2104.
42. Bialy, L., and Waldmann, H. (2004). Total synthesis and biological evaluation of the protein phosphatase 2A inhibitor cytostatin and analogues. Chem. Eur. J. *10*, 2759–2780.
43. Bialy, L., and Waldmann, H. (2002). Synthesis of the protein phosphatase 2A inhibitor (*4S, 5S, 6S, 10S, 11S, 12S*)-cytostatin. Angew. Chem. Int. Ed. *41*, 1748–1751.
44. Bialy, L., and Waldmann, H. (2003). Synthesis and biological evaluation of cytostatin analogues. Chem. Commun. *15*, 1872–1873.
45. Bhatt, U., Christmann, M., Quitschalle, M., Claus, E., and Kalesse, M. (2001). The first total synthesis of (+)-ratjadone. J. Org. Chem. *66*, 1885–1893.
46. Watanabe, Y., Ishikawa, S., Takao, G., and Toru, T. (1999). Radical cyclization on solid support: synthesis of γ-butyrolactones. Tetrahedron Lett. *40*, 3411–3414.
47. Kim, S.W., Hong, C.Y., Lee, K., Lee, E.J., and Koh, J.S. (1998). Solid phase synthesis of benzylamine-derived sulfonamide library. Bioorg. Med. Chem. Lett. *8*, 735–738.
48. Thutewohl, M., and Waldmann, H. (2003). Solid-phase synthesis of a pepticinnamin E library. Bioorg. Med. Chem. *11*, 2591–2615.
49. Thutewohl, M., Kissau, L., Popkirova, B., Karaguni, I.-M., Nowak, T., Bate, M., Kuhlmann, J., Müller, O., and Waldmann, H. (2002). Solid-phase synthesis and biological evaluation of a pepticinnamin E library. Angew. Chem. Int. Ed. *41*, 3616–3620.
50. Kondoh, M., Usui, T., Kobayashi, S., Tsuchiya, K., Nishikawa, K., Nishikiori, T., Mayumi, T., and Osada, H. (1998). Cell cycle arrest and antitumor activity of pironetin and its derivatives. Cancer Lett. *126*, 29–32.
51. Kondoh, M., Usui, T., Nishikiori, T., Mayumi, T., and Osada, H. (1999). Apoptosis induction via microtubule disassembly by an antitumor compound, pironetin. Biochem. J. *340*, 411–416.
52. Usui, T., Watanabe, H., Nakayama, H., Tada, Y., Kanoh, N., Kondoh, M., Asao, T., Takio, K., Watanabe, H., Nishikawa, K., et al. (2004). The anticancer natural product pironetin selectively targets Lys352 of α-tubulin. Chem. Biol. *11*, 799–806.
53. Mayer, T.U., Kapoor, T.M., Haggarty, S.J., King, R.W., Schreiber, S.L., and Mitchtison, T.J. (1999). Small molecule inhibitor of mitotic spindle bipolarity identified in a phenotype-based screen. Science *286*, 971–974.
54. Haggarty, S.J., Mayer, T.U., Miyamoto, D.T., Fathi, R., King, R.W., Mitchison, T.J., and Schreiber, S.L. (2000). Dissecting cellular processes using small molecules: identification of colchicine-like, taxol-like and other small molecules that perturb mitosis. Chem. Biol. *4*, 275–286.
55. Miyamoto, D.T., Perlman, Z.E., Mitchison, T.J., and Shirasu-Hiza, M. (2003). Dynamics of the mitotic spindle – potential therapeutic targets. Prog. Cell Cycle Res. *5*, 349–360.
56. Pelkmans, L., Fava, E., Grabner, H., Hannus, M., Habermann, B., Krausz, E., and Zerial, M. (2005). Genome-wide analysis of human kinases in clathrin- and cavaeolae/raft-mediated endocytosis. Nature *436*, 78–86.